

Morphology Variety and Formation Mechanisms of Polymeric Membranes Prepared by Wet Phase Inversion

Č. STROPNIK,* L. GERMIČ, and B. ŽERJAL

Faculty of Chemistry and Chemical Engineering, University of Maribor, 2000 Maribor, Slovenia

SYNOPSIS

The cross-section morphologies of polymeric membranes obtained by scanning electron microscopy are presented. Membranes are prepared by a wet phase inversion process from cellulose acetate, polysulfone, polyester and a polyether type of elastomeric polyurethanes, poly(methylmethacrylate), and polyamide—nylon 4,6. Morphologies are qualitatively correlated with the turbidity appearance and its intensity during the (proto)membrane formation process and with their permeability to pure water. From the morphological characteristics, such as different cellular or dense structures, macrovoids, and polymer beads, and from the turbidity phenomena during the (proto)membrane formation, the nucleation and growth of polymer-lean or polymer-rich phase and the spinodal modes of polymer–solvent–nonsolvent ternary system decomposition are postulated. © 1996 John Wiley & Sons, Inc.

INTRODUCTION

Loeb and Sourirajan's pioneer article¹ opens a path to an extensive development in the field of polymer membrane technology and science. Some of the books^{2–12} published in this field give the impression about the extent of the research and development work already done. At the same time, numerous technological applications of polymeric membranes in different industries, in medicine, in environmental protection, just to mention some of most propulsive fields, take place; they are in constant spread and growth.

Many preparation methods for polymeric membranes have been discovered and/or developed so far. One of the most useful methods is membrane preparation by a phase inversion process: thermodynamic instability has to be somehow induced in the solution of the polymer, which turns by some process(es) into the polymer (proto)membrane. In the case of a wet phase inversion process, the cast solution of polymer is put in lasting contact with the liquid nonsolvent for polymer (coagulation bath);

mass transfer of the solvent and nonsolvent brings the solution of polymer to the necessary thermodynamic instability. The (proto)membrane is formed by its resolution, accompanied by the obligatory solidification of the polymer. A broad variety of morphologically very different polymer membranes can be prepared by changing the parameters of the wet phase inversion process (polymer, solvent, nonsolvent, composition of polymer solution and coagulation bath, additives, temperature, etc.). Recently, some useful empirical rules dealing with the polymeric membrane formation processes are turning into the proposals for membrane formation mechanisms;^{13–29} they are based on deeper understanding of the phenomena of the polymer membrane formation processes.

The present work shows a broad morphological variety of membranes prepared by a wet phase inversion process from different polymer/solvent systems; in all cases, the coagulation bath is pure water. Turbidity phenomena occurring during the membrane formation process and membrane permeabilities to pure water under ultrafiltration conditions are also presented. At the end, some membrane formation mechanisms consisting of the combination of some elementary processes are proposed. A qualitative description of elementary processes by their

This article is dedicated to the memory of Breda Žerjal.

* To whom correspondence should be addressed.

Journal of Applied Polymer Science, Vol. 61, 1821–1830 (1996)

© 1996 John Wiley & Sons, Inc.

CCC 0021-8995/96/101821-10

“composition paths” in the polymer–solvent–non-solvent ternary phase diagram is also presented.

EXPERIMENTAL

The following polymers were used for membranes preparation: cellulose acetate (CA; Merck 11,1962, acetate content 39,8 wt %, $M_w = 30,000$ D, $T_g = 240^\circ\text{C}$), polysulfone (PSf; Aldrich 18,244–3, $M_w = 30,000$ D, $T_g = 190^\circ\text{C}$), elastomeric thermoplastic polyurethane of polyester type (TPU1; BASF, Elastollan C90 A), elastomeric thermoplastic polyurethane of polyether type (TPU2; BASF, Elastollan 1190 A), poly-(methylmethacrylate) (PMMA; Aldrich 18,226–5, $M_w = 120,000$ D, $T_g = 110^\circ\text{C}$) and polyamide (PA4,6; Nylon4,6, Stanyl KS400). The solvents used were acetone for CA, *N,N*-dimethylacetamide (DMA) for PSf, *N,N*-dimethylformamide (DMF) for both TPUs and for PMMA, and formic acid for PA4,6; solvents had the reagent grade purity. Solutions of polymer were prepared by weighting components and mixing them long enough (24–48 h) so that clear solutions were formed.

Polymer solutions were cast on the grinded glass plate (unevenness of the surface of the grinded glass plate was $\pm 3 \mu\text{m}$; it was determined by a visible light interference measurement and independently by a mechanical measurement with an OPTON instrument) by square knives with the exactly dimensioned slit D (the slit dimension D was taken as the nominal thickness of the cast solution; dimensions of slits were also determined with an OPTON instrument with the exactness of $\pm 3 \mu\text{m}$); the plate with the cast solution of polymer was immersed into the coagulation bath with pure water at 25°C as quickly as possible (3–5 s). The onset, speed of increase, and maximal value of the turbidity of the casting solution/(proto)membrane system were measured by a photoresistor, amplifier, and recorder (a turbidity measurement setup).^{18,25,30} The (proto)-membranes thus formed were left in the coagulation bath for 10–15 min before being transported into the vessel with a slightly agitated large quantity of water; they remained under such conditions for the next 24–48 h.

For the characterization of the cross-section morphology by the scanning electron microscopy (SEM, JEOL JSM-840A) the membrane was dried for at least 24 h between the filter paper, frozen in liquid nitrogen, broken, mounted into the sample holder, gilded, and examined with SEM.

The membrane permeability to pure water was determined by measuring the water flux through the

membrane in the AMICON 8400 cell under the ultrafiltration pressure of nitrogen.

RESULTS AND DISCUSSION

Polymeric Membrane Formation Process by Wet Phase Inversion

The preparation of polymer membranes by a wet phase inversion process consists of three main parts: Pr casting of the solution of polymer on the appropriate support; glass (or metal) plate with or without some reinforced material (nonwoven polyester, e.g.) is usually used in research experiments; Pr immediate immersion of the cast solution of polymer into the coagulation bath; particularly when the solvent in the casting solution has its boiling point not much above the temperature at which the casting takes place, the transfer of cast solution has to be done as quickly as possible (within a few seconds); if not, the evaporation of the solvent leads to the “dry/wet phase inversion process,” because the evaporation time has considerable effects on the ultimate membrane structure.^{14,15,20,27,28,31} Pr post treatment of the (proto)membrane formed; it is usually left in the coagulation bath for some time (5–30 min) and then rinsed with water for a longer period (24–48 h); in some cases, some temperature annealing of (proto)-membrane is carried out.

We worked with “historical” polymer membrane materials such as cellulose acetate (CA) and polysulfone (PSf). Further, we worked with poly(methylmethacrylate) (PMMA) and polyamide, nylon4,6 (PA4,6), which are also known as materials for membrane preparation. On the other hand, we also worked with two different (polyether and polyester type) elastomeric thermoplastic polyurethanes (TPU1 and TPU2), just recently commercially available. Their detailed constitution is still under the manufacturer’s embargo.

In the membrane preparation we limited ourselves to a “pure” three-component system: casting solutions always consisted of pure solvent and polymer, without addition of nonsolvent or any other additive(s); coagulation bath was a one-component system, for instance, pure water in all cases.

During the immersion step of the membrane preparation with the wet phase inversion process, we also qualitatively followed some turbidity phenomena: appearance (instantaneous, delayed), its speed of increase, and its maximal value. After the immersion of the cast solution of polymer into the coagulation bath, the mass transfer of nonsolvent

into the polymer solution and of solvent into the coagulation bath began. This process usually leads to a thermodynamically metastable and/or unstable ternary system. This instability is resolved by some kind of decomposition process. Especially the nucleation and growth demixing process, which appeared in metastable solutions, produced the objects on which the light could be intensively scattered; the cast solution/(proto)membrane system became turbid. Therefore, the turbidity phenomena give us some information about the beginning and intensity of decomposition process(es) during the membrane formation by wet phase inversion.

We also determined the characteristics of prepared membranes by measuring the pure water fluxes under ultrafiltration conditions. The membrane permeability as a performance characteristic in combination with other characteristic(s) should give some ideas about the porosity (of a part) of membranes.

Morphology, Turbidity Phenomena, and Permeability of Prepared Membranes

Figure 1 represents the cross-section morphology of the membrane prepared from the CA/acetone : water system; $300\ \mu\text{m}$ was the nominal thickness of the 20 wt % cast solution of CA in acetone. Although the nominal layer thickness and the concentration of the cast solution are relatively high, the formed membrane is very thin in comparison with other below-presented membranes (see magnification bars). (Round) cells are clearly visible on the upper half of the membrane, while the lower part consists of the formless polymer mass; the cellular structure is poorly developed and has no evident interconnections. On the coagulation bath–membrane interface (upper part on Fig. 1) a very compact structure can be seen; this is the skin of the membrane. Turbidity phenomena occurring during the CA membrane formation process are quite characteristic (Table I): the delay of the onset of turbidity is about 17–23 s, the speed of turbidity increase is high, and the maximal value of turbidity is low. The CA membrane is not permeable for pure water under ultrafiltration conditions (Table I).

Morphologies of membranes, prepared from the ternary system PSf/DMA : water [Fig. 2(a)–(c)] are quite different in comparison with the morphology of the CA membrane. PSf membranes also have pronounced differences in morphology among themselves. Great parts of membranes, where the polymeric material is absent, are obvious. In Figure 2(a), these parts of the membrane look as channels



Figure 1 SEM micrographs of the cross-section of the CA membrane; 20 wt %, $300\ \mu\text{m}$.

leading from the top to the bottom; the lower part of the membrane is a large cavity and on the bottom there is a well-developed cellular structure. Figure 2(b) and (c) show membranes with voids in the shape of a “long tear,” which are called in the polymeric membranes literature “finger-like structures” or “macrovoids.” Qualitatively, it could be estimated that in Figure 2(c) the number of macrovoids per unit of membrane length is smaller and that they are shorter than the macrovoids in the membrane prepared from a $200\ \mu\text{m}$ thick and 21 wt % PSf solution [Fig. 2(b)]. If we compare the “nonpolymer” parts of all three PSf membranes, it is obvious that the channels on the membrane of 12.5 wt %/ $100\ \mu\text{m}$ turn to macrovoids when the concentration and the thickness of the casting solution is increased to 30 wt %/ $300\ \mu\text{m}$. The “nonmacrovoid” part of membranes consists of a well-developed cellular structure; cells are bigger in Figure 2(c) than in Figure 2(b). As it is the case with the CA membranes, the turbidity phenomena are also characteristic for the PSf membranes (Table I): the instantaneous onset of turbidity, high speed of its increase and a high maximal value of its intensity. The membrane with a channel-like morphology [Fig. 2(a)] has extremely high permeability to water while “macrovoid membranes” [Fig. 2(b) and (c)] are practically impermeable to water under ultrafiltration conditions (Table I).

Table I Results of Turbidity and Water Flux Measurements

SEM	Polymer Solution wt %/Thickness ^a	Turbidity Phenomena			Water Flux (l/m ² h) (Bar)
		Onset	Speed of Increase	Maximal Value	
Figure 1	CA/acetone 20/200	delay	high	low	none
Figure 2(a)	PSf/DMA 12,5/100	instantaneous	high	medium	730 (2) 1080 (4)
Figure 2(b)	PSf/DMA 21/200	instantaneous	high	high	none
Figure 2(c)	PSf/DMA 30/300	instantaneous	high	high	none
Figure 3(a)	TPU1/DMF 20/200	instantaneous	high	low	1,6 (4)
Figure 3(b)	TPU2/DMF 20/200	instantaneous	high	low	2,2 (4)
Figure 4	PMMA/DMF 20/300	without any turbidity			22 (2)
Figure 6(a, b)	PA4,6/HCOOH 30/300	very slight delay	slow	medium	95 (0,5)

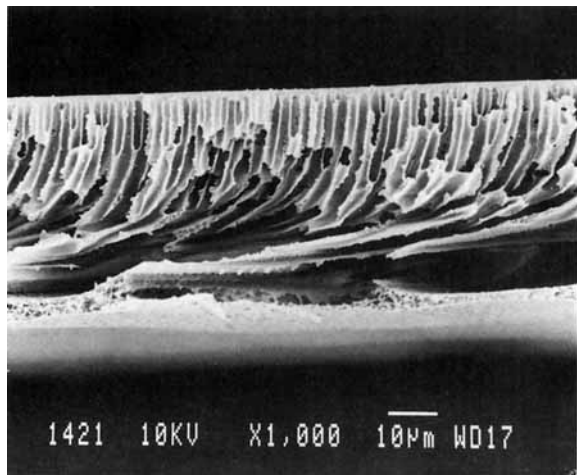
^aIn micrometers; CA—cellulose acetate; PSf—polysulfone; TPU—thermoplastic polyurethan; PMMA—poly(methylmetacrylate); PA4,6—polyamide 4,6; DMA—*N,N*-dimethylacetamide; DMF—*N,N*-dimethylformamide.

Even larger “tear-like” macrovoids are formed in membranes prepared by the wet phase inversion from the TPU1/DMF : water and TPU2/DMF : water systems [Fig. 3 (a) and (b)]. The morphology of these membranes consists almost entirely of macrovoids. Most of them extend from the top to the bottom of the membrane where a well-developed cellular structure with relatively small cells can be found. Macrovoid walls also consist of the cellular structure when they become thicker in the lower part of the membranes. Turbidity measurements (Table I) show instantaneous onset of turbidity, high speed of its increase, and low maximal value. Water fluxes through both TPUs membranes are relatively small under ultrafiltration conditions (Table I).

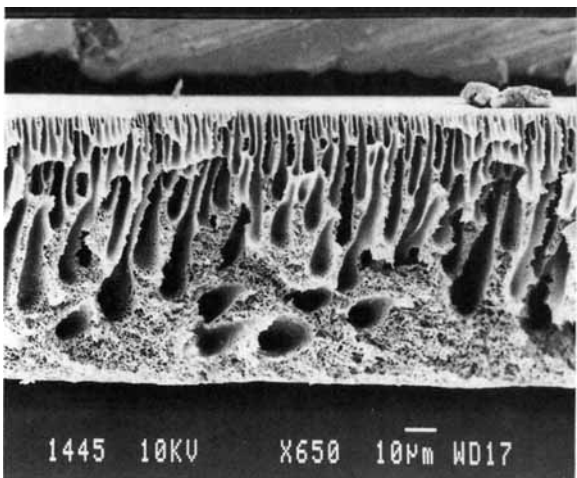
A completely different morphology is obtained in the case of the membrane preparation from the PMMA/DMF : water system (Fig. 4); it looks almost like a “dense” membrane. But close inspection of the SEM micrograph shows some shadows and even cavities, holes, and crevices on the matrix of the “dense” polymer material. Figure 5 also shows the morphology of the PMMA membrane. All three micrographs represent the same membrane but snapped at different magnifications and after increasing time of exposure of the membrane to the electron beam. As the magnification and the exposure time increase, the polymer begins to melt and

interesting bicontinuous structure is formed: an interconnected three-dimensional network of the solid polymer and accordingly interconnected caves and holes [Fig. 5 (b) and (c)]. The turbidity phenomena of the PMMA/DMF cast solution/(proto) membrane system are also special: no turbidity appearance was detected even under the greatest amplification of the turbidity measurement setup; only small opaqueness was detected visually. Under the ultrafiltration conditions relatively high-water permeability was observed for, on the first sight, “dense” PMMA membrane (Table I).

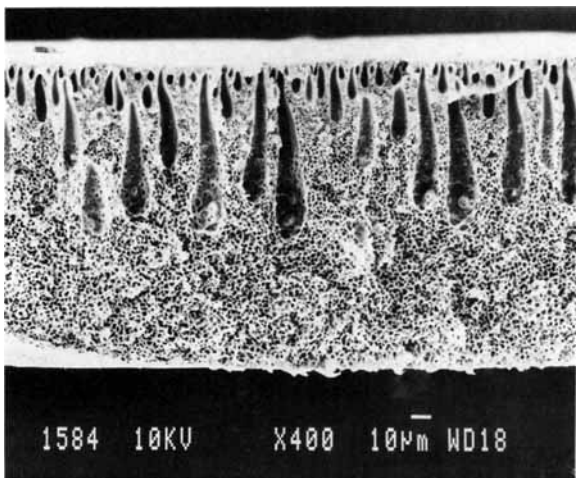
The morphology of the membranes prepared from the PA4,6/formic acid : water system [Fig. 6(a) and (b)] is somehow akin to membranes from PMMA: a kind of “dense” structure with more expressed holes, cavities, and crevices. But besides these resemblances, the polymeric material in the PA4,6 membranes is accumulating at some places into globular forms so that the shape of the polymer beads can be distinguished. The greatest difference between the PMMA and the PA4,6 membranes formation process concerns the turbidity phenomena: the cast solution/(proto) membrane system does not show any turbidity at all in the case of PMMA while in the case of PA4,6 the turbidity has a slight delay (of a few seconds), slow speed of increase, and medium maximal value (Table I). The PA4,6 membrane has a quite thick but not very dense skin. Its



(a)



(b)



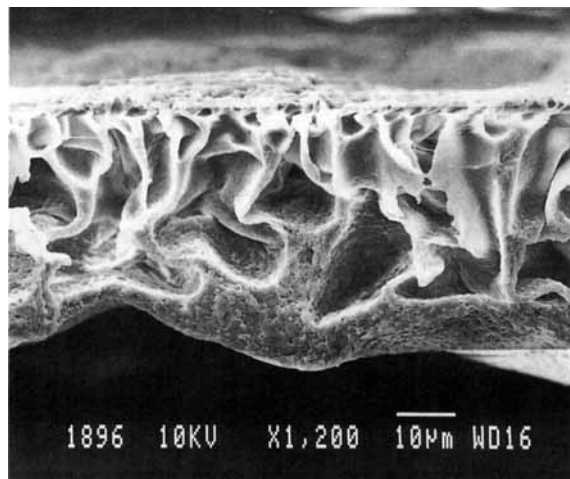
(c)

Figure 2 SEM micrographs of the cross-sections of the PSf membranes; (a) 12.5 wt %, 100 µm; (b) 21 wt %, 200 µm; (c) 30 wt %, 300 µm.

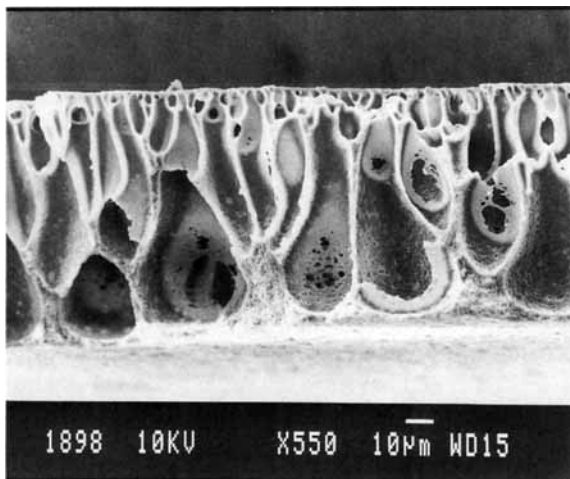
permeability to water under ultrafiltration conditions is very high (Table I).

“Composition Paths” and Elementary Processes of Membrane Formation Mechanism

Changes in the composition of the polymer–solvent–nonsolvent system produced by mass transfer of a nonsolvent into cast solution and of a solvent into the coagulation bath during polymeric membrane preparation by wet phase inversion can be schematically represented in the ternary phase diagram by a “composition path.” In Figure 7, the ternary phase diagram for polymer–solvent–nonsolvent is presented. The arrows numbered from 1 to 4 represent some distinguishing changes in composition of the liquid ternary system. The same numbers are attached to the rectangles under the ternary phase



(a)



(b)

Figure 3 SEM micrographs of the cross-section of the TPU1 and TPU2 membranes; (a) 20 wt % TPU1, 200 µm; (b) 20 wt % TPU2, 200 µm.

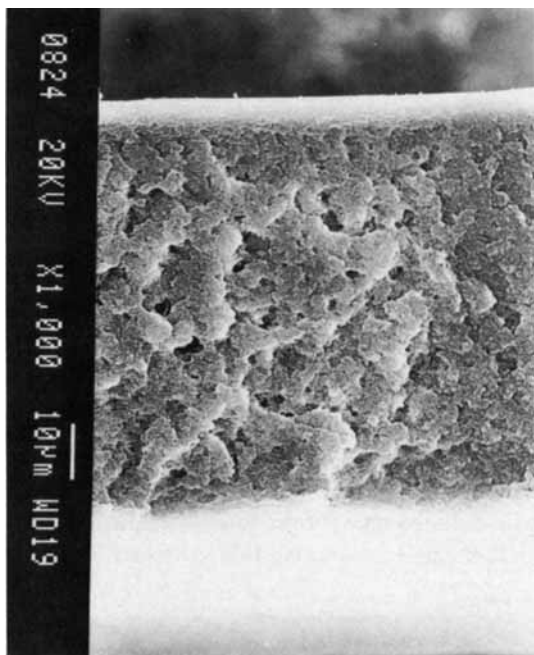
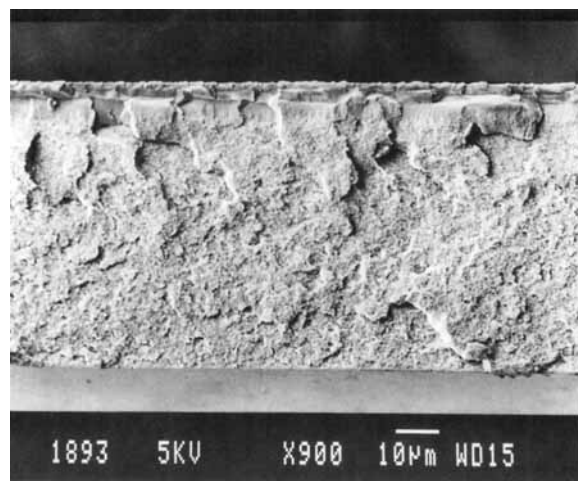


Figure 4 SEM micrographs of the cross-section of the PMMA membrane; 20 wt %, 300 μm .

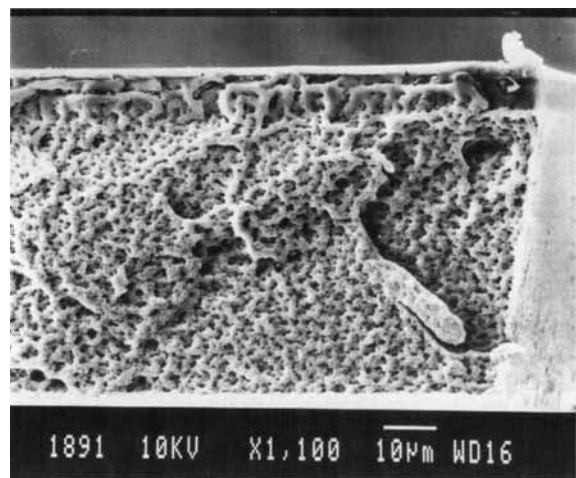
diagram where the structures, formed by distinguishing "composition paths," are schematized; hatched areas represent the solid polymer.

The "composition path 1" means that the concentration of the polymer in the more and more viscous ternary system is increasing because the outflow of the solvent from the cast solution/(proto) membrane system is faster than the inflow of the nonsolvent into the same system; the entangled polymer molecules solidify by gelation and/or by "glass transition" and/or by crystallization into a dense, compact structure.^{21,22} It is clear that at such "phase transition" there is no turbidity appearance because no objects capable to scatter light are formed. It could also be expected that such a dense structure is practically impermeable to water under ultrafiltration conditions. An analogous "phase transition" is taking place at the solidification of the polymer-rich phase when it is formed by any mode of ternary solution decomposition described below; but it is not necessary that the mode of solidification for a given polymer-solvent-nonsolvent system should be the same on the both sides of the binodal.

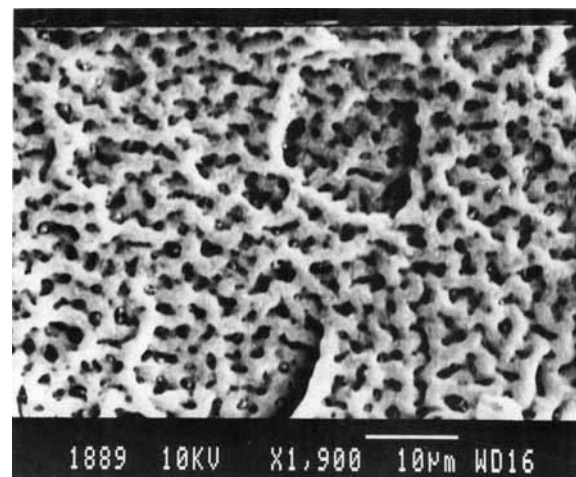
The "composition path 2" (a relative speed of solvent and nonsolvent mass transfer is analogous to the case of "composition path 1") means that the ternary polymer solution becomes metastable. If the concentration fluctuations enable the formation of



(a)



(b)



(c)

Figure 5 SEM micrographs of the cross-sections of the PMMA membranes, snapped in time interval; (a) original membranes 20 wt %, 300 μm ; (b) after 2 min; (c) after 6 min.

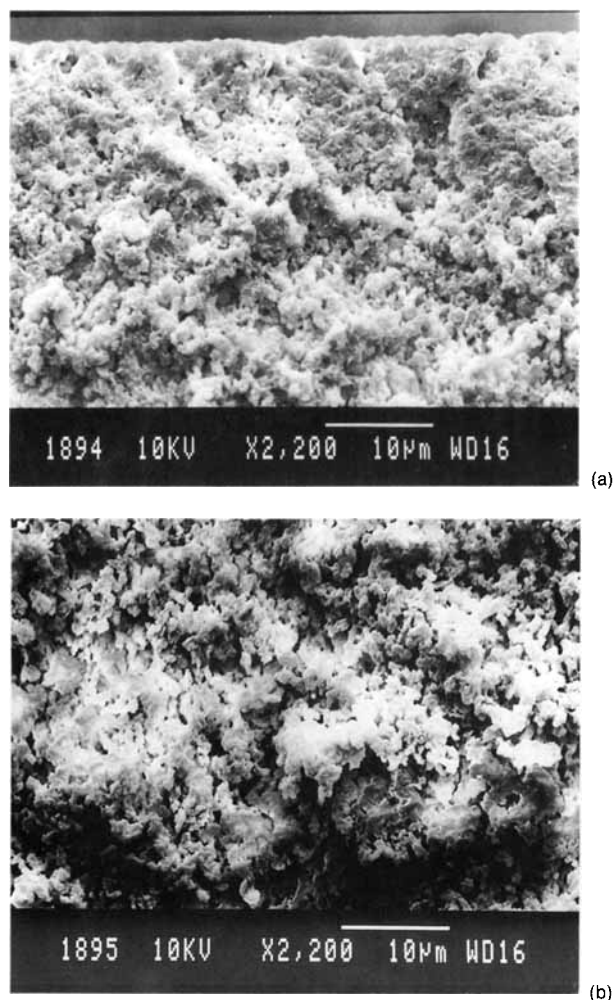


Figure 6 SEM micrographs of the cross-sections of the PA4,6 membranes; (a) 30 wt %, 300 μm ; (b) another part of the same membrane.

sufficiently big nuclei, with the composition connected by the tie line to the binodal on the opposite side of the miscibility gap, the nuclei of the polymer-lean phase can begin to grow. The phase inversion as the process of nucleation and growth of the polymer-lean phase begins. The nuclei grow until the surrounding polymer-rich phase solidifies and a more or less developed cellular structure is formed. Intensive light scattering and, consequently, turbidity appear; its speed of increase depends on the speed of the nuclei formation, and its intensity depends on the number and size of the nuclei. In the case of interconnected cells, a small resistance to water flux can be expected.

The “composition path 3” means that the ternary polymer solution becomes unstable and even small concentration fluctuations induce the phase inversion process. By spinodal demixing of the ternary

polymer solution the polymer-rich and the polymer-lean phases are formed; their compositions are, again, determined by tie lines. The fundamental characteristic of spinodal demixing is continuous and gradual change of composition and, consequently, a slow growth of the quantity of both phases; they are interconnected within themselves and form a three-dimensional bicontinuous network.³²⁻³⁴ As in the previous cases, the polymer-rich phase also solidifies here by some mode of solidification when the concentration of the polymer increases over certain limits. No formation of objects capable of light scattering is present and, consequently, no turbidity appearance at all is expected when the decomposition of the ternary polymer solution takes place by means of spinodal demixing. Because of the inherent interconnectivity of the polymer-lean phase, which is leached out in the subsequent process of membrane formation, a great water flux through such spinodal polymer structure should be expected.

The “composition path 4” means that the formation of the nuclei of the polymer-rich phase in the matrix of the polymer-lean phase takes place. Only when the concentration of nuclei and the speed of their growth are big enough so that the beads thus formed stick together, the compact polymer membrane is formed;²⁹ otherwise, the polymer latex is formed. As it is the case with the “composition

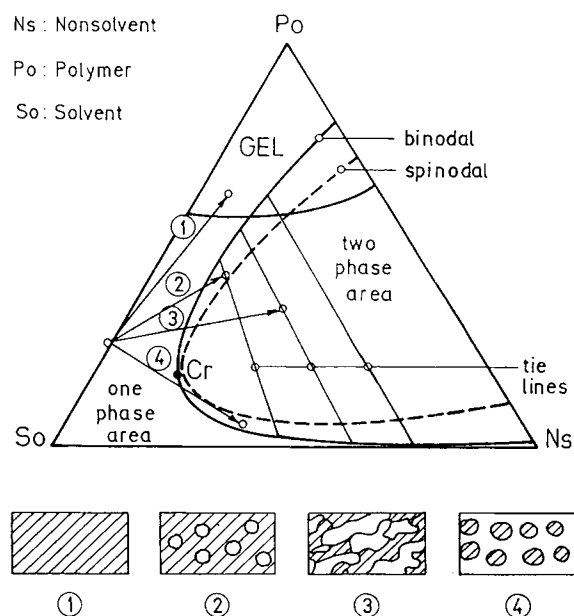


Figure 7 Ternary phase diagram polymer-solvent-nonsolvent with directions of distinguished “composition paths”; 1—solidification, 2—nucleation and growth of the polymer-lean phase, 3—spinodal demixing, 4—nucleation and growth of the polymer-rich phase.

path 2,” the turbidity appearance also takes place because of the light scattering on the formed nuclei. The permeation of water through such packed structure of the polymer beads is expected to be very high.

Polymeric Membranes Formation Mechanism

The mechanism of the membrane formation from the “pure” CA/acetone : water system is a combination of the “composition path 1” and the “composition path 2.”²⁴ After the immersion of the cast solution into the coagulation bath, the concentration of the polymer in the ternary solution is increased because the outward (acetone) mass transfer is greater than the inward (water) one. After some time, the nuclei of the polymer-lean phase are formed; thus, the turbidity appears with some delay. During the delay the CA/acetone : water system shrinks considerably because the ultimate CA membrane is the thinnest among the described ones. It is very probable that membrane skin will be formed during this process. The speed of turbidity increase is high because of the abrupt appearing of the nuclei of the polymer-lean phase. Its maximal value is low because the number of nuclei in a volume unit is not high; they also appear only on the upper part of the membrane. So the CA membrane has a poorly developed cellular structure (“composition path 2”), which remains after the leach out of the polymer-lean phase. Under ultrafiltration conditions there is no water flux through the CA membrane.

Membranes prepared from the “pure” PSf/DMA : water system [Fig. 2(a)–(c)] are formed by mechanism(s) that we cannot explain into every detail. The channels [Fig. 2(a)] and macrovoids [Fig. 2(b) and (c)] are the morphological objects, the formation of which could not be explained simply by any of the previously described “composition paths” or their combination. Some other effects^{35,36} like the intrusion of the nonsolvent,^{37,38} the coalescence of nuclei of a polymer-lean phase,^{17,25} and Marangoni’s effects,^{14,16,23} to mention just some of them, are probably operative either alone or as a combination during the formation of the membranes from the PSf/DMA : water system. The turbidity phenomena appearing during this membrane formation process have a clear explanation in their morphology: the nucleation and growth of the polymer-lean phase (“composition path 2”) starts immediately after the immersion of the cast solution and the turbidity onset occurs instantaneously; very quick appearance of nuclei is responsible for the high speed of turbidity increase, and a very large nuclei population is re-

sponsible for the high maximal value of turbidity. The nucleation and growth process is stopped by the solidification of the surrounding polymer-rich phase. These processes are reflected in a very well-developed cellular structure that remains after the leach out of the polymer-lean phase. The permeability to water under ultrafiltration conditions is extremely high for the membrane with a channel structure [Fig. 2(a)] and vanishes in the case of membranes with macrovoids [Fig. 2(b) and (c)]; it is evident that the upper layer of the membrane (the skin) and/or the absence of the cell’s interconnectivity are responsible for no water permeability.

The excellent “wholly macrovoid membranes” are prepared from both TPU/DMF : water systems [Fig. 3(a) and (b)]. The study of formation of membranes with such well-shaped macrovoids, especially in the case of the polyether type of TPU [Fig. 3(b)], can serve for an explanation of the macrovoid formation mechanism(s). The turbidity phenomena appearing during the TPUs membrane formation are in some aspects akin to those of the PSf and those of the CA membranes: the onset is instantaneous and the speed of increase is high; its maximal value is low. The immediate and abrupt formation of a large number of nuclei of the polymer-lean phase is the reason for the instantaneous appearance of turbidity, for its high speed of increase, and for a large number of very small cells; the reason for the low maximal turbidity is the fact that the part of the membrane with a cellular structure is very small. In spite of the “wholly macrovoid structure,” which suggests great permeability possibilities, the TPUs membranes allowed a relatively low water flux under ultrafiltration conditions; this is a further evidence that the skin of the membrane is decisive for its permeability.

Membranes prepared from the PMMA/DMF : water system [Figs. 4 and 5(a)] have a completely different morphology. We believe that the formation of such a structure is a consequence of the spinodal demixing of the ternary polymer solution (“composition path 3”) with the subsequent solidification of the polymer-rich phase. An evidence for the spinodal decomposition is also a complete absence of turbidity phenomena during the PMMA membrane formation process. A relatively high water flux under ultrafiltration conditions through such a morphologically “dense” membrane suggests also the interconnectivity of the cavities remaining after the leach out of the polymer-lean phase; due to the spinodal demixing, the polymer-lean phase as well as the polymer-rich phase are interconnected into a three-dimensional bicontinuous network. The further ev-

idence for such a statement is given in Figure 5 (a), (b), and (c). In Figure 5 (a), the morphology of the PMMA membrane is presented; by a further magnification [Fig. 5 (b) and (c)] the electron beam interacts with the gilded membrane so strongly that the heat effects begin to melt the polymer; the thinnest and finest parts of the continuous solidified polymer-rich phase began to melt and by surface decreasing coalesce on the thicker and massiver parts of the continuous solidified polymer-rich phase. So the altering of the original structure of the PMMA membrane is small and the SEM micrographs strongly reveal its original spinodal structure. The formed pattern excellently fits the theoretically predicted pattern for spinodal demixing.^{32,34}

The morphology of the membrane, prepared from the PA4,6/formic acid : water system also suggests the spinodal demixing of the ternary polymer solution. But the turbidity phenomena are contestable: a slight delay (of a few seconds) of the onset, slow speed of the turbidity increase, and the medium maximal value of turbidity are their main characteristics. Some relatively slow nucleation and growth process takes place during the PA4,6 membrane formation process. The morphology of the membrane with poorly developed polymer globules (beads) and a slow nucleation process [mass transport of the polymer (segments) is expected to be a slower process than the mass transport of the solvent and nonsolvent] suggest the demixing of the ternary polymer solution by the nucleation and growth of the polymer-rich phase. Thus, the formation mechanism of the PA4,6 membrane is a combination of the spinodal demixing ("composition path 3"), nucleation and growth of the polymer-rich phase ("composition path 4") and a subsequent solidification of the polymer-rich phase. The very high water flux through the PA4,6 membrane could be an auxiliary evidence for the proposed decomposition of the ternary polymer solution by above proposed mechanism.

CONCLUSION

The morphology of membranes prepared by the wet phase inversion reflects the mechanism of their formation: the nucleation and growth process of the polymer-lean and also polymer-rich phase, the process of spinodal demixing of the polymer-solvent-nonsolvent ternary system, and the process of solidification of the concentrated polymer solution (gelation and/or "glass transition" and/or crystal-

lization) are clearly represented in SEM micrographs.

A poorly or well-developed cellular structure in the CA, PSf, and TPUs membranes reflects the polymer-lean phase nucleation and growth; the process of growth is stopped by the solidification of the surrounding polymer-rich phase and accomplished by a subsequent leach out of the polymer-lean phase from the cells. A "dense" structure of the PMMA membranes with some cavities, holes, and crevices in their polymer matrix (bicontinuous structure) reflects the spinodal demixing with further solidification of the interconnected network of the polymer-rich phase. In the case of the PA4,6 membranes, an agglomerated polymer, much alike to beads, reflects the polymer-rich phase nucleation, growth, and solidification in the "background" of spinodal demixing.

These processes also reflect the turbidity phenomena occurring during the membrane formation by a wet phase inversion process: the nucleation and growth of any phase is always accompanied by a substantial increase in turbidity of the cast solution / (proto)membrane system, while due to the spinodal demixing of the system, there is practically no appearance of turbidity. The delayed or instantaneous onset of turbidity is reflected in the thickness of the membrane and in the poorly or well-developed cellular structure; the speed of turbidity increase reflects the mass transport of polymer (segments) or solvent and nonsolvent during the nucleation and growth of the polymer-rich or polymer-lean phase, respectively; and its maximal value reflects the poorly or well-developed cellular and beads structure.

The formation of channels and especially macrovoids as prominent morphological features of PSf and TPUs membranes takes place by a mechanism that we cannot explain.

It is not suitable to predict the permeability of membranes for water from their morphology; it depends to a large degree on the uppermost part of the membrane—its skin—which is usually so thin that SEM micrographs revealing the whole cross-section of the membranes could not show details important for the membrane permeability. But relatively high water permeabilities of membranes from PMMA and from PA4,6 should reveal their formation by spinodal demixing (bicontinuous structure) and by nucleation and growth of polymer-rich phase (packed beads), respectively.

The authors wish to express their gratitude to Prof. Dr. A. Krizman for making accessible the SEM in his labo-

ratory and to T. Bončina for her excellent and patient work on our membranes.

REFERENCES

1. S. Loeb and S. Sourirajan, *Adv. Chem. Ser.*, **38**, 117 (1962).
2. M. H. V. Mulder, *Basic Principles of Membrane Technology*, Kluwer Academic Publishers, Dordrecht, 1992.
3. Y. Osada and T. Nakagawa, Eds., *Membrane Science and Technology*, Marcel Dekker, New York, 1992.
4. R. Rautenbach and R. Albrecht, *Membrane Processes*, John Wiley and Sons, Chichester, 1985.
5. B. Sedlaček and J. Kohovec, Eds., *Synthetic Polymeric Membranes*, Walter de Gruyter, Berlin, 1987.
6. P. M. Bungay, H. K. Lonsdale, and M. N. de Pinho, Eds., *Synthetic Membranes: Science, Engineering and Applications*, D. Reidl Publishing Company, Dordrecht, 1986.
7. S. Sourirajan and T. Matsuura, Eds., *Reverse Osmosis and Ultrafiltration*, American Chemical Society, Washington, DC, 1985.
8. D. R. Lloyd, Ed., *Material Science of Synthetic Membranes*, American Chemical Society, Washington, DC, 1985.
9. R. E. Kesting, *Synthetic Polymeric Membrane*, John Wiley, New York, 1985.
10. A. F. Turbak, Ed., *Synthetic Membranes*, Vols. I and II, American Chemical Society, Washington, DC, 1981.
11. H. Strathmann, *Trennung von molekularen Mischungen mit Hilfe synthetischer Membranen*, Dr. Dietrich Steinkopf Verlag, Darmstadt, 1979.
12. S. Sourirajan, Ed., *Reverse Osmosis and Synthetic Membranes, Theory, Technology, Engineering*, National Research Council Canada, Ottawa, 1977.
13. S. S. Shojaie, W. B. Krantz, and A. R. Greenberg, *J. Membr. Sci.*, **94**, 255 (1994).
14. S. S. Shojaie, W. B. Krantz, and A. R. Greenberg, *J. Membr. Sci.*, **94**, 281 (1994).
15. W. B. Krantz, R. J. Ray, and R. L. Sani, *J. Membr. Sci.*, **29**, 11 (1986).
16. F. G. Paulsen, S. S. Shojaie, and W. B. Krantz, *J. Membr. Sci.*, **91**, 265 (1994).
17. C. A. Smolders, A. J. Reuvers, R. M. Boom, and I. M. Wienk, *J. Membr. Sci.*, **73**, 259 (1992).
18. P. Radovanovic, S. W. Thiel, and S. T. Hwang, *J. Membr. Sci.*, **65**, 213 (1992).
19. C. S. Tsay and A. J. McHugh, *J. Polym. Sci., Part B: Polym. Phys.*, **28**, 1327 (1990).
20. C. S. Tsay and A. J. McHugh, *J. Membr. Sci.*, **64**, 81 (1991).
21. G. E. Gaides and A. J. McHugh, *Polymer*, **30**, 2118 (1989).
22. W. R. Burghardt, L. Yilmaz, and A. J. McHugh, *Polymer*, **28**, 2085 (1987).
23. A. J. Reuvers, J. W. A. van den Berg, and C. A. Smolders, *J. Membr. Sci.*, **34**, 45 (1987).
24. A. J. Reuvers and C. A. Smolders, *J. Membr. Sci.*, **34**, 67 (1987).
25. A. J. Reuvers, Ph.D. Thesis, University Twente, Enschede, Netherlands, 1987.
26. R. J. Ray, W. B. Krantz, and R. L. Sani, *J. Membr. Sci.*, **23**, 155 (1985).
27. S. C. Peseck and W. J. Koros, *J. Membr. Sci.*, **81**, 71 (1993).
28. I. Pinnau and W. J. Koros, *J. Appl. Polym. Sci.*, **43**, 1491 (1991).
29. D. R. Lloyd, *J. Membr. Sci.*, **52**, 239 (1990).
30. R. M. Boom, Th. van den Boomgard, and C. A. Smolders, *J. Membr. Sci.*, **90**, 231 (1994).
31. B. Kunst and S. Sourirajan, *J. Appl. Polym. Sci.*, **14**, 1983 (1970).
32. J. W. Cahn, *J. Chem. Phys.*, **42**, 93 (1965).
33. C. A. Smolders, J. J. van Aartsen, and A. Steenberg, *Kolloid Z. Z. Polym.*, **243**, 14 (1971).
34. M. Konno, Y. Nishikori, and S. Saito, *J. Chem. Eng. Jpn.*, **26**, 33 (1993).
35. L. Zeman and T. Fraser, *J. Membr. Sci.*, **84**, 93 (1993).
36. L. Zeman and T. Fraser, *J. Membr. Sci.*, **87**, 267 (1994).
37. H. Strathmann, K. Kock, and P. Amar, *Desalination*, **16**, 179 (1975).
38. H. Strathmann and K. Kock, *Desalination*, **21**, 241 (1977).

Received September 29, 1995

Accepted December 29, 1995